Multi-material distributed recycling via Fused granular fabrication: rHDPE and rPET case of study

Catalina Suescun Gonzalez[1], Hakim Boudaoud[1], Cécile Nouvel[2], Fabio A. Cruz Sanchez[1], Joshua Pearce[3]

[1]Université de Lorraine – ERPI – F-54000, Nancy, France
[2]Université de Lorraine –LGPI – F-54000, Nancy, France
[3]Western University, Department of Electrical & Computer Engineering, Canada, London

Abstract

The high volume of plastic waste and the extremely low recycling rate has created a serious challenge worldwide. Local distributed recycling coupled to additive manufacturing (DRAM) offers a solution by economically incentivizing local recycling. A new DRAM technology capable of processing large quantities of plastic waste quickly is fused granular fabrication (FGF), where solid shredded plastic waste can be reused directly as 3D printing feedstock. This study presents an experimental assessment of multi-material recycling printability, using two of the most common thermoplastics in the beverage industry polyethylene terephthalate (PET) and high-density polyethylene (HDPE) and the feasibility of mixing PET and HDPE to be used as a feedstock material for large-scale 3-D printing. After the material collection, shredding, and cleaning its characterization, and optimization of parameters for 3D printing was performed. Results showed the feasibility of printing a large object from rPET/rHDPE flakes reducing the production cost up to 88%. .

1 Introduction

The disposal of plastic waste is one of the most challenging current environmental concerns given its systemic complexity (Evode et al., 2021). The mass of micro- / meso- plastics in the oceans are expected to exceed the mass of the global stock of fish by 2050 (MacArthur, 2017). More critically, the global plastic annual production is expected to reach 1100 metric tons by the same year (Geyer, 2020). The societal awareness on plastic recycling have received substantial attention by scientific, policymaker and general public (Soares et al., 2021). Unfortunately, the statistical analysis on the centralized recycling process proves that it has been largely ineffective (Siltaloppi and Jähi, 2021) as only 9% of the plastic that has been produced has been recycled from the total stock produced since 1950 (Geyer et al., 2017). Therefore, it remains an open challenge to identify alternatives to valorize discarded plastic material.

Distributed recycling and additive manufacturing (DRAM), is an innovative technical approach to recycle plastic wastes (Cruz Sanchez et al., 2020; Dertinger et al., 2020). DRAM was first practiced with recyclebots, which are waste plastic extruders that made filament for conventional fused filament-based 3-D printers (Baechler et al., 2013; Woern et al., 2018; Zhong and Pearce, 2018). Past research demonstrated that using distributed recycling fits into the circular economy paradigm (Despeisse et al., 2017; Ford and Despeisse, 2016); where consumers directly recycle their own waste into consumer products from open source designs, from toys for children (Petersen et al., 2017) to adaptive aids for those with arthritis (Gallup et al., 2018). Distributed manufacturing is now in wide use (Pearce and Qian, 2022). In this way DRAM-based recycling is done in a closed loop supply chain network (Santander et al., 2020). This type of recycling aims to reduce the environmental impact by the reduction of the transportation from the waste source to recycling facilities (M. A. Kreiger et al., 2014). In that sense, it aims to propose innovative closed-loop strategies using waste materials as raw resources (Romani et al., 2021).

Fused filament fabrication (FFF, which is also known as Fused Deposition Modelling –FDM©-

) is the most-widespread and established extrusion-based AM technology due to the open source proliferation from the self-replicating rapid prototyper (RepRap) project (Bowyer, 2014; Jones et al., 2011; Sells et al., 2009). This is due to its simplicity, versatility, low-cost, and ability in the construction of geometrically complex objects in the industrial and prosumer domains (Romani et al., 2021). Indeed, the open-source 3-D approach for 3-D printers has enabled the technology to evolve in a radical manner for manufacturing and prototyping adding value to the recycled material (Cruz Sanchez et al., 2020). There are large efforts to find sustainable feedstocks for 3-D printing Pakkanen et al. (2017a). Several studies in the literature have increase the spectrum of recycled filament materials such as PLA (Anderson, 2017; Cruz Sanchez et al., 2017a), ABS (Mohammed et al., 2017b, 2017a), PET (Vaucher et al., 2022; Zander et al., 2018), HDPE (Baechler et al., 2013; Chong et al., 2017; Mohammed et al., 2017b) PC (Gaikwad et al., 2018). In fact, using a comparative life cycle assessment in a low density population case study of Michigan, USA, M. a. Kreiger et al. (2014) argued that about of 100 billion MJ of energy per year could be saved in a distributed approach, for the 984 million pounds of HDPE that are recycled in the U.S. There is thus considerable evidence that DRAM can reduce the energy consumption and greenhouse gases of the manufacturing processes.

Most DRAM studies have been using mono-material for the fabrication of feedstock for FFF. There are, however, several examples of mixed materials including wood waste and recycled plastic (Löschke et al., 2019; Pringle et al., 2018) and textile fibers and recycled plastic (Carrete et al., 2021). Recently, Zander et al. (2019) reported the manufacturing of composite filament from recycled PET/PP and PS/PP blending through compatibilizer copolymer such as SEBS. Their results revealed the technical printability of polypropylene blend composite filaments from a thermo-mechanical characterization perspective. Increasing the performance window of blending materials by compatibilization which could be a relevant path for recycling plastics in a local level and isolated areas contexts (e.g. during humanitarian crises (Savonen et al., 2018 ; Corsini et al., 2022 ; Lipsky et al., 2019), supply chain disruptions (Attaran, 2020; Choong et al., 2020 ; Novak and Loy, 2020; Salmi et al., 2020) and/or isolated

off-grid situations using solar-powered 3-D printers (Gwamuri et al., 2016 ; King et al., 2014; Mohammed et al., 2018; Wong, 2015)). Likewise, Vaucher et al. (2022) studied the evaluation of the microstructure, mechanical performance, and printing quality of filaments made from rPET and rHDPE varying the wt% of HDPE material from 0 to 10%. They confirmed the increase in the Young's modulus from 1.7 GPa of the pure PET to 2.1 GPa for all the HDPE concentrations. Additionally, the maximum stress of the bends were augmented with high HDPE concentrations. Values were lower than virgin PET filament, yet similar to commercial recycle ones. The addition of rHDPE at higher levels, however, helped to meet the brittle-ductile transition in 15% despite the low interfacial tension of both polymers, allowing the printing of quality parts.

While former studies have proven been successful in FFF, a new approach to DRAM is fused granular fabrication (FGF) or fused particle fabrication (FPF), where the material-extrusion AM systems print directly from pellets, granules, flakes, shred or grinder material (Fontana et al., 2022; Woern et al., 2018). In the context of recycling, this could reduce the number of melt/extrusion cycles that degrade the material needed in the filament fabrication process (Cruz Sanchez et al., 2017b). The FGF technique opens up the potential of use recycle materials as well as print large-scale objects either with a conventional cartesian 3-D printer (Woern et al., 2018), delta 3-D printer (Grassi et al., 2019) or hangprinter Rattan et al. (2023). Research groups corroborate that plastic waste can be used as feedstock materials for FGF/FPF. Alexandre et al. (2020) assessed the technical and economical dimensions of virgin and shredded PLA printed in a self-modified FGF machine and compared with FFF. The investigation showed that the use of FGF reduced printing cost, time and its mechanical performance was comparable with the obtained using the traditional FFF technique. Likewise, Woern et al. (2018) found comparable properties between PLA, ABS, PP, and PET recycled and virgin materials. Later publications demonstrated the technical and economic feasibility through the printing of complex objects validating the possibility of recycle plastic with FGF in both conventional and common FFF materials (Byard et al., 2019), but also recycle PC (Reich et al., 2019) and rPET (Little et al., 2020,). Few

researchers, however, have addressed the problem of the direct printing of recycled multi-materials, which might be a key step forward needed to facilitate the ease of sorting and recycling post-consumer plastic waste materials.

This study explores the potential of direct 3-D printing two immiscible polymers commonly used in the beverage sector through a distributed recycling process for its easily implementation operation at the local level. To demonstrate the feasibility of the process, the bottled water plastic most used in France of roughly 90% of PET (body of the bottle) and 10% of HDPE (cap) now called *rPET90//rHDPE10*, is used as a test material. The experimental process of collection, characterization, and printing of the recycled material is described and the results are discussed in the context of widespread DRAM adoption at the community level.

2   Materials and Methods

The methodology presented in Figure 1 outlines the approach adopted to develop the study. The four stages *Material*, *Material preparation*, *Printing process* and *Evaluation* were thoroughly studied in order to control the major processes steps and the technical characterization methods. In the following subsections, each step is explained.
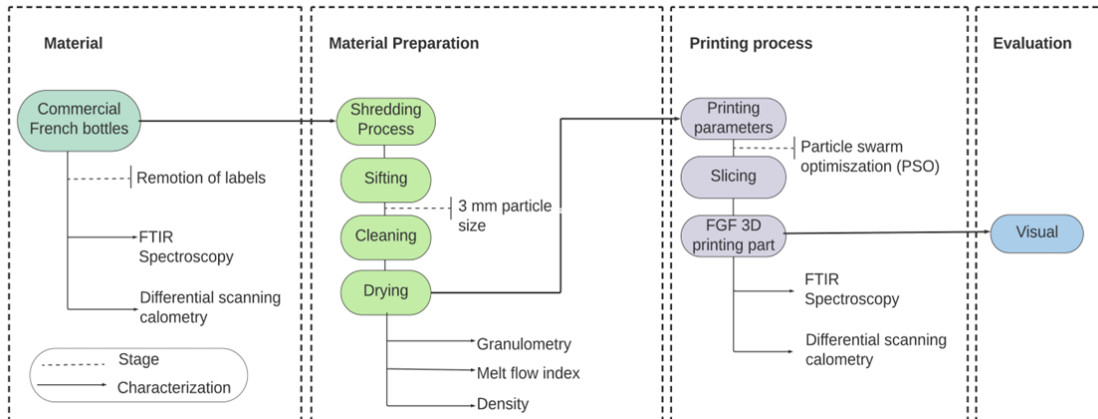

Figure 1: Global framework of the study

2.1 Raw material obtention

The goal of material stage is the collection of post-consumer plastic source. In this study, water of bottles coming from the French brand Cristaline was used as a feedstock. A framework of the process used is shown in Fig. 1.a. Post-consumer bottles were collected by receptacles placed in partnership schools in Lorraine, France. To convert the complete water bottles with its cap into 3DP feedstock material, the labels were removed before shredding in a cutting mill Retsch MS300 using a 3 mm grid. After shredding, the obtained flakes were sifted with a 3 mm sifter. Next, they were cleaned with hot water in an ultrasonic machine at 60°C for 1h to remove contaminants. Lastly, they were dried in a conventional oven overnight at 80°C (Taghavi et al., 2018; Van de Voorde et al., 2022) to avoid degradation of the material. Washing conditions were the same for all the samples, therefore, the effect of contaminants was not considered. The resultant material is shown in Fig. 1.b.

Figure 2: figure1

The material composition was calculated as a function of the mass of the bottles and caps separately. The percent (%) of bottle-cap was found to be ~90%rPET and ~10% rHDPE. The complete bottle was shredded without separation of both materials thus this percentage is constant for all the samples.

2.2 Material preparation

2.2.1 Material particle size analysis -Granulometry-

In order to ensure the particle size suitable for printing, the characterization of the granulate particles were developed using the open-source ImageJ software (ImageJ, 2023). The size characteristics of the particles were evaluated between four different samples; vPET (used as a reference) and the raw material sifted in three different sizes 1.5 mm, 3 mm and 5 mm.

2.2.2 Fourier-transform infrared spectroscopy –FTIR-

FTIR spectroscopy was carried out to determine the nature of the bottle and determine if there were impurities, plasticizers or additives that could be detected. The analysis were made on samples of rPET and rHDPE separately and then a printed sample of both materials to determine if there was possible to observe a chemical bonding. Every sample was measured in two different points, three times in each point then curves were normalized and analyzed with the Origin Pro 8 (**https://www.originlab.com/origin?**). The Fourier transform infrared spectra have been recorded in the range of 4000 cm^{-1} to 375 cm^{-1} with resolution 4 cm^{-1} using Bruker IFS 66V spectrophotometer.

2.2.3 Differential scanning calorimetry –DSC-

Differential scanning calorimetry analysis were performed with a DSC-1 Mettler Toledo with STARe software operating under nitrogen atmosphere at heating rate and cooling rate of 10 $°C/min$. rPET, rHDPE and rPET90//rHDPE10 samples were investigated using three cycles: first heating from 20°C to 270 °C, cooling to 20 °C and reheating to 270°C. The rHDPE sample was analyzed following similar cycles but with the maximum temperature set at 250°C and pBC with temperatures from -20 to 270°C. Glass transition temperature (Tg) of rPET was determined during the first heating cycle, while rPET90//rHDPE10 (Tg) during the second heating cycle along with the melting point of all materials. Crystallization temperature (Tc) of the each of the materials was determined during the cooling cycle. The degree of crystallinity (Xc) was calculated from the second cycle for recycled materials and

first cycle for the blend as expressed in equation (1) (Pan et al., 2020; Taghavi et al., 2018):

$$X_c(\%) = \frac{\Delta H_m}{w \cdot \Delta H_m^\circ} \tag{1}$$

Where, ΔH_m is the latent heat of melt, w is weight percentage of polymer in the blend, and ΔH_m° is the reference heat of 100% crystalline PET (140 J/g) and HDPE (293 J/g), respectively, provided in the literature (Kratofil et al., 2006; Pan et al., 2020).

2.2.4 Melt Flow Index −MFI-

The melt-flow index (MFI) of rPET90//rHDPE10 flakes was determined using a Instron CEAST MF20. The analysis was performed using three samples of ~5 g at 255 °C using a 2.16 kg weight according to ASTM D1238. The process was repeated three times. The average value of the three results was then reported with $gr/10 \times min$ unit.

2.2.5 Density

In order to calculate the material's density, first; the volume was found measuring the dimensions of a solid $50x50x50$ mm cubic geometry fabricated injecting rPET90//rHDPE10 flakes into a square mould with a known volume using open-source desktop injection (Holipress, Holimaker, France) machine. Then the model was weighed, and the mass was obtained. Finally, density was calculated as expressed in Equation 2. To ensure the accuracy the test was performed twice and the average value was reported in g/cm^3.

$$\rho = V/m \tag{2}$$

Where, ρ is the density, V is the volume, and m the mass.

Afterwards, experimental results were compared with the theoretical blend density which could be calculated by Equation 3.

$$\rho_{12} = \frac{1}{\frac{W_1}{\rho_2} + \frac{W_2}{\rho_2}}$$

(3)

Where, ρ_{12} is the density of the blend, W_1 and W_2, the weight fractions of each polymer, ρ_1 and ρ_2, the theoretical density of each polymer for PET (1.38 g/cm^3) and HDPE 0.93 to 0.97 g/cm^3 (Jonathan GUIDIGO1 et al., 2017).

2.3   Printing process

2.3.1   Establishing optimal parameters

Establishing optimum combinations of parameters is essential for better quality and mechanical properties of the printed parts (Jaisingh Sheoran and Kumar, 2020). According to Oberloier et al. (2022a), particle swarm optimization (PSO) is an effective and time-effective method for this purpose. The optimization of the 3-D printing parameters for the rPET90//rHDPE10 material in the GigabotX was performed using the open-source PSO Experimenter platform (available in Linux), following the methodology developed by Oberloier et al. (2022a). Three process benchmark artifacts were printed; line, plane, and cube. They were modeled in CAD software Onshape CAD v1.150 and sliced using Prusaslicer v2.52.0. The geometry models and dimensions are shown in Fig. 2.

Geometry	Lenght (mm)	width (mm)	height (mm)
Line	200	2	1
Plane	100	100	1
Cube	40	40	40

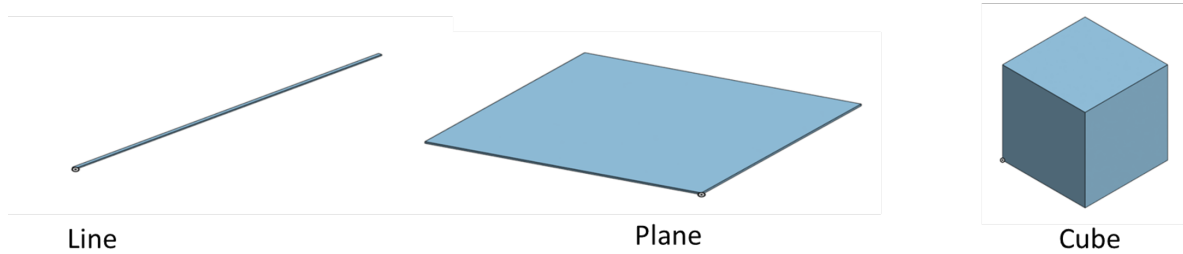Line   Plane   Cube

Figure 3: Dimensions and CAD models of the geometries used for parameters optimization.

Four parameters were assessed: 1) the nozzle temperature, 2) bed temperature, 3) the printing

Table 1: table 1

(a) Line optimization initial parameters

Variable	Min	Max	Guess	True/False	Description
T1	255	270	260	TRUE	Temperature Zone 1 on GigabotX
Tb	80	90	85	TRUE	Bed temperature
Ps	10	25	15	TRUE	Printing Speed
E	0.5	2	1	FALSE	Extrusion Multiplier

(b) Fixed parameters to perform printing parameters optimization based on PSO

Parameters	Value	Units
Layer height	0.5	mm
Width	2	mm
T2	230	°C
T3	220	°C
Cooling	0	%
Infill density	2	%

(c) Recommended parameters for PSO tuning

Variable	Value	Description
Kv	0.5	The emphasis given to the velocity component
Kp	1.0	The emphasis given to a particle's personal best position
Kg	2.0	The emphasis given to the swarm's group best position

speed and 4) extrusion multiplier (Oberloier et al., 2022b). The initial parameters for the line are presented in Table 1 while other parameters were obtained in preliminary experimental work shown in Table 1.b. Finally, the PSO tuning parameters were found in the previous PSO work (Oberloier et al., 2022a) Table 1.c.

2.3.2 Fused Granular Fabrication –FGF-

To print the raw material obtained, a 3-heat-zone modified open-source printer (Gigabot XL re:3D, Houston, TX, USA) was used. The machine is a single screw extrusion-based 3-D printer capable of direct printing pellets, flakes or granules, with a nozzle size of 1.75 mm. For this study, a chair was printed to evaluate the ability for the material to 3-D print and the machine capacity to print large-objects such as a piece of furniture. The ideal parameters found for the cube geometry were used to print the final part.

3   Results and discussion

3.1   Material characterization

Both polymeric components of the bottle as well as the blend were characterized and analyzed to determine their properties using different methods as explained in the previous section.

3.1.1   Material particle size analysis (granulometry)

The material after shredding has an irregular shape, which led to machine clogging and generated under-extrusion issues, lowering the quality of the prints. Therefore, granulometry evaluation is essential to control these issues. Previous studies demonstrated that particles with areas smaller than 22 mm^2 were optimal for print without jamming or under-extrusion problems (Woern et al., 2018). From the experiments conducted, however, particles with areas above 10 mm^2 clogged in the feeding system and auger screw of the machine. Therefore, granulometry analysis was performed using three different mesh sizes.

Figure 4 shows the results obtained, where particles sifted at 5 mm had an average area similar to the reference. There are, however, particles with areas over 9 mm^2 which blocked in the feeding and extrusion section. Particles sifted to 1.5 mm showed a distribution with areas from 0 to proximately 3 mm^2, this area was considered too low for printing. Small particles can completely melt in the first heat zone obstructing the consistent flow of other particles and not allowing the pressure needed to extrude the melted particles lower in the screw. Although flakes of 3 mm show a more dispersed distribution and slightly lower area compared with the reference, those particles were found to be optimal for printing. The final objects, however, still displayed under-extrusion issues. For this reason, a crammer was implemented (Little et al., 2020); which physically pushes particles to the auger to convey them from feeding tube into the extruder. After the crammer implementation under-extrusion issues were significatively decreased. It was concluded that flakes with areas between 1.5 mm^2 to 10 mm^2 were optimum for print using a crammer able to aid the feeding system.
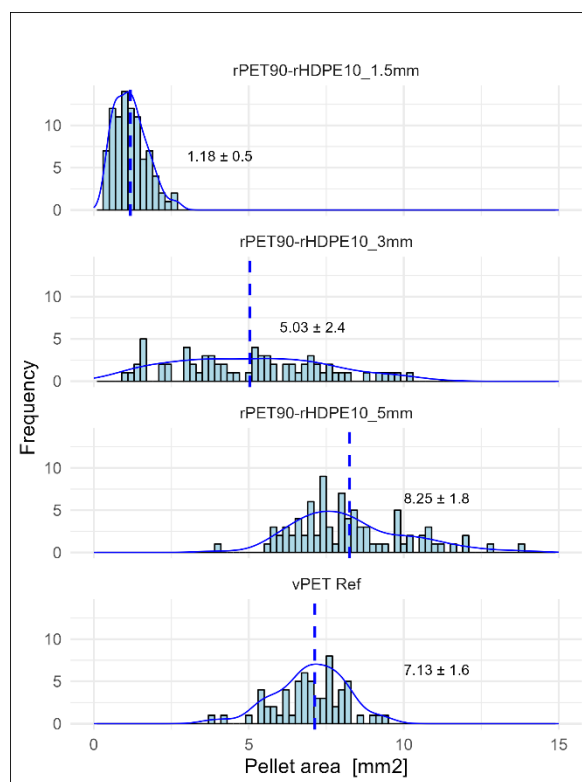
Figure 4: Granulometry analysis

3.2 Chemical analysis from FTIR

Chemical structure information of the materials was obtained using FTIR spectroscopy, which provided analysis of the characteristic spectral bands of the polymers. First, for the rPET (bottle) four characteristic bands can be observed Fig 4, one in $1713cm^{-1}$ representing the $C = O$ double bond, the $C-O$ single bond ester at $1240cm^{-1}$, $1093cm^{-1}$ band corresponding to the methylene group and vibrations of the ester bond and finally, a band $722cm^{-1}$ the CH2 rocking bending vibration.

Similar results were obtained in the literature for PET coming from recycled water bottles, soda bottles and food containers (Zander et al., 2018). For rHDPE (caps), four characteristic peaks were observed, the bond of C-H functional group in peaks $2915cm^{-1}$ and $2847\ cm^{-1}$, main bending mode of the -CH2 in $1465\ cm^{-1}$ and CH2 rocking bending vibration at $729\ cm^{-1}$. These results confirmed the chemical structures of starting materials. Additionally, other indicative resonances besides those associated with the polymer structures were not observed, concluding that additives or plasticizers in significative quantities were not present in either sample. The spectrum of the printed blend (rPET90//rHDPE10) had the same characteristic peaks as the bottle, confirming the PET dominant content. There are, however, observable differences between $1000\ cm^{-1}$ and $720\ cm^{-1}$ and in the bond of C-H ($2915\ cm^{-1}$ and $2847\ cm^{-1}$ peaks), confirming the presence of HDPE (cap). The shifting observed can be attributed to the hydrogen interactions between both materials.

3.3 Thermal analysis DSC

The thermal properties of both recycled materials and their blend were characterized via DSC to have a starting point for the 3-D printing process parameter optimization.

From the representative heating and cooling thermograms shown in Fig. 5, two distinct endothermic peaks are observed in the printed blend sample that are associated with fusion of the crystalline fractions of rHDPE and rPET, which confirms the immiscibility of both materials. Moreover, a significant reduction in the enthalpy of fusion and crystallization of
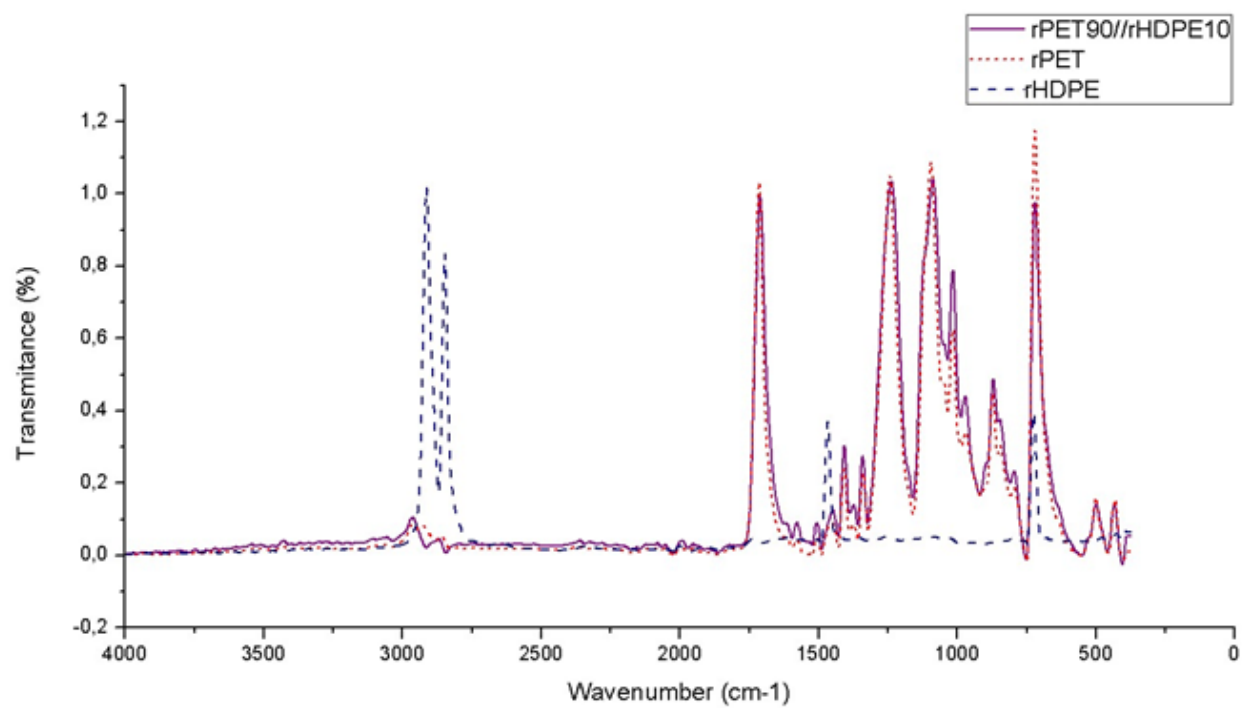
Fig.4. FTIR spectra of rPER, rHDPE and their blend

Figure 5: FTIR spectra of rPET, rHDPE and their blend

Table 2: Thermal analysis of rPET, rHDPE and their blend

Sample	Glass transition Tg (°C)	Melting Tm (°C)	Melting ΔHm (J/g)	Crystallization Tc (°C)	Crystallization ΔHc (J/g)	Crystallization ΔHcc (J/g)	% Crystallinity Xc
rPET	82	249.9	31.6	196.7	34.8	-	22.6
rHDPE	-	133.8	172	118.7	158.5	-	58.7
rPET90/rHDPE10	77 / -	254/131.7	40.3/1.30	210.6/117.4	37.9/6.7	6.8	24.8 / 18.4

the rHDPE in the blend is attributed to the low percentage of HDPE in the blend. The observation of cold crystallization peak in the blend but not in the individual polymers, however, can be attributed to an interaction between both polymers, where the rHDPE might act as a nucleating agent. Table 2. list the thermal properties for rPET, rHDPE and rPET90//rHDPE10. The melting point for rHDPE and rPET are 131.7 °C and 249.9 °C, respectively and are similar to those found in the literature (Chen et al., 2015; Lei et al., 2009; Vaucher et al., 2022). It is observed that the melting and crystallization temperature of rPET shifted to a higher value, while slightly decreasing for rHDPE. In addition, the crystallization of rPET was found to be somewhat affected by the addition of rHDPE as it was increased 4%. It is likely the addition of the rHDPE acted as germination point for crystallization (Vaucher et al., 2022). The slight changes in the rPET temperatures of fusion-crystallization and degree of crystallinity showed the interaction of both polymers.

3.4 Rheology MFI

The melt flow index of the flakes was determined, enabling a fast and practical screening of the viscosity of the material. Following the DSC results, the initial temperature to start the MFI test was 250°C, however the material did not flow reliably so the temperature was increased by 5°C to enable the melt flow index of the rPET90//rHDPE10 to be determined. A temperature of 260°C was also tested, however, the material flowed rapidly and the measurement could not be reliably obtained. MFI tests were performed three times and the results of the rPET90//rHDPE10 was a medium MFI 39.4± 2.4 g/10min, which is roughly consistent with values found in literature for rPET (Bustos Seibert et al., 2022; Nofar and Oğuz, 2019; Salminen?). This result suggests that the low percentage addition of HDPE do not highly
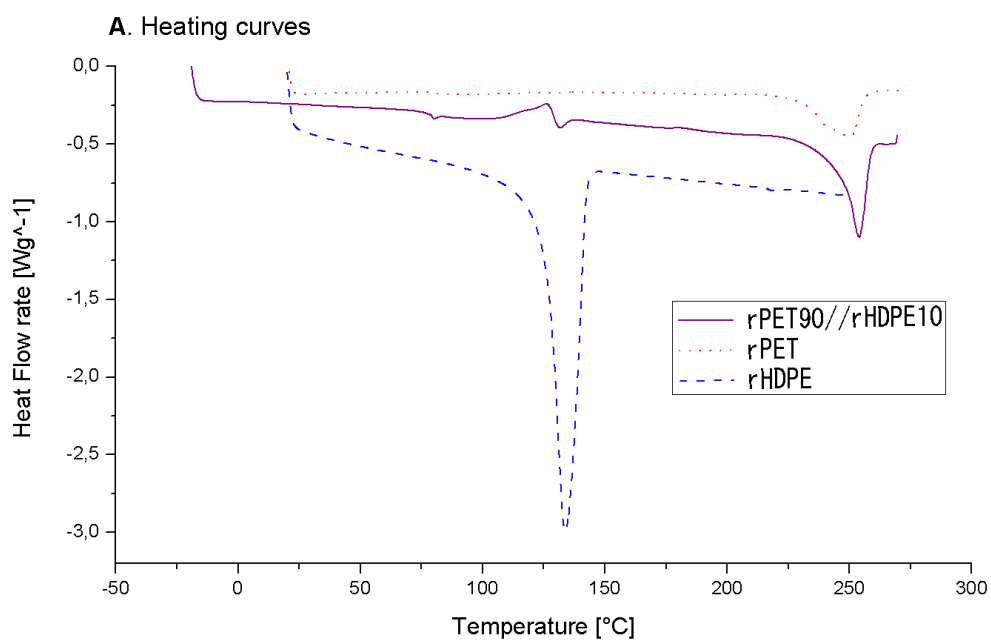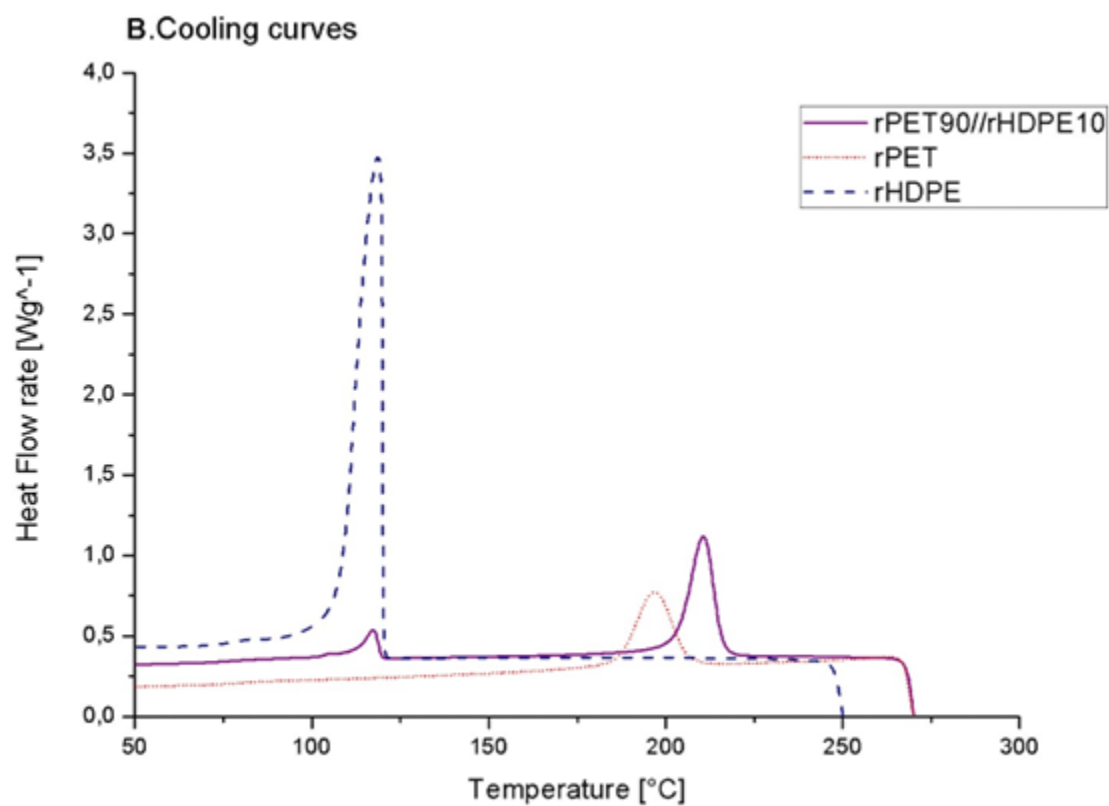
(a) Heating curves

(b) Cooling curve

Figure 6: DSC thermograms of recycled materials and blends

impact the MFI value of rPET. As the material flowed at temperature of 255°C in the MFI, it provided the input temperature for 3-D printer parameters optimization.

3.5 Density

The density allows the estimation of cost, material use, time consumed and weight of the printing object in the slicer. This information is useful to find the accurate printing parameters with the PSO experimenter as fitness is calculated as a function of the dimensional accuracy and weight of the printed object. Hence, density was useful to determine the weight of the geometries.

From calculations made after weight and measuring the rPET90//rHDPE10 injected object, the density of the material was found to be 1.13 g/cm^3. The inclusion of HDPE in the matrix polymer led to a slight decrease in its density, which is a common outcome when a polymer is mixed with a lower density polymer. However, if we consider a PET/HDPE blend with a mass ratio of 90/10, the calculated theoretical density is 1.32 g/cm^3. The observed decrease of 14% in the results could be attributed to factors such as experimental conditions and manual measurements

3.6 Particle swarm optimization (PSO) Experimenter

Geometries were 3-D printed changing the parameters as expressed in the PSO Experimenter software. The fitness function is defined by the weighted sum of the dimensional measurements (length, width, height, and weight) of the printed object, where fitness below 0.1 was set as a desirable threshold. In the software five particles were established for one iteration, thus in one iteration five different parameters combinations were printed. The first geometry (line) was able to reach a fitness of < 0.1 after six iterations for a total of thirty lines printed. The ideal parameters for this geometry are listed in column two of Table 3.

Afterwards, these parameters were used as initial guess for plane geometry, which reached the desired fitness in the first iteration. Likewise, cubes were printed using the plane ideal

parameter as initial guess and optimal parameters, where found in the first iteration. Results showed a significant change in the printing speed, which lowers at higher geometry complexity. Moreover, the cube geometry required a higher extrusion multiplier to fill gaps and overcome under-extrusion problems. The optimization of the parameters for the three geometries took around 10h reducing the experimental time, compared with conventional methods. According to Oberloier et al. (2022a) this time of experimentation can be reduced 97%. Indeed, the efficacity of PSO in finding global optimum parameters is high, particularly when there is a large or complex design space (Saad et al., 2019; Selvam et al., 2020).

Additionally, PSO converge to optimum solutions with fewer iterations that DoE methods (Zhang et al., 2015) while mixing PSO with other meta-heuristic methods has shown higher ability of predict and optimize parameters (e.g. minimize surface roughness(Shirmohammadi et al., 2021), compressive strength and porosity of scaffolds (Asadi-Eydivand et al., 2016), mechanical properties(Raju et al., 2019)). However, the DoE methods are still widely used as they provide insight into the effects of individual design parameters and their interactions while the ability to find interaction between the variables is not possible using PSO. In the beginning of a set of optimization experiments, the complete understanding of the process technique as well as the function settings might be complex. The methodology used in this study, however, was easy to implement and the software has the advantage of being free, open source and user-friendly, lessening the initial difficulty. Thus, PSO demonstrated to be an effective and high accuracy prediction technique able to find the initial optimum parameters for rPET90//rHDPE10 material for FGF/FPF.

From the results it is observe that the optimal parameters may change depending of the object printed and each parameter has its own variation. One hypothesis is that geometry might play a role in parameter assignment and probably could be more visible in larger prints, yet this hypothesis needs further investigation. There are several physical mechanisms at play that would be expected to change optimal printing parameters based on the geometry and size of the object. For example, the cooling time and temperature history of a voxel will depend on the geometry of the printed object. Thus, to maintain the same thermal history

Table 3: Ideal printing parameters for fused granule fabrication of waste PET and HDPE blend made from shredded whole plastic water bottles

Variable	Line value	Planes value	Cube value	Δ	Units
T1	258	263	264	6 $\pm$3.2	°C
Tb	86	82	84	4$\pm$2	°C
Ps	21	14	10	11$\pm$5.6	mm/s
E	1.07	0.87	1.32	0.5$\pm$0.3	-

the printing parameters must change as the geometry changes. This same effect of thermal history can also have more subtle impacts such as degree of crystallization even for PLA (Wijnen et al., 2018).

In addition, some physical effects of materials extrusion are magnified with scale. The most obvious is the impacts of thermal expansion and contraction. Small changes in contraction as a part cools may cause acceptable distortions for small prints, but these are magnified for large prints (e.g. causing deformation and in the worst cases delamination or loss of bed adhesion)(Shah et al., 2019). Although, Roschli et al. (2019) showed the obstacles and possible solutions of the large-scale AM according to the way of the parts are designed the incidence of the geometry in the printing parameters needs far more detailed future studies. Specifically better models for mapping 3-D printing parameter optimizations of small printed objects to large volume objects is needed.

Table 3. Ideal printing parameters for fused granule fabrication of waste PET and HDPE blend made from shredded whole plastic water bottles.

3.7 Functional object print

The ideal parameters found for the cube geometry were used as final parameters for print the case study product, except the print speed for the optimized line speed was used to decrease the printing time and delamination. This change was performed as according to the PSO results the material is printable in a range of 10 to 20 mm/s. Additionally, the faster the printing the lesser the time of cooling between the layers thus avoiding possible delamination

(Roschli et al., 2019), which is exacerbated for larger objects.

The Gigabot X successfully produced a piece of furniture from multi-material recycled water bottles that included mixing HDPE and PET as shown in Fig. 6.a.

The printing quality is acceptable as a prototype, proven the machine capacity of printing large-scale functional objects where the chair was able to hold a child with a mass of 20 kg comfortably as shown in Fig.6 f. The material, in the other hand, needs further evaluation as the printed object showed weak bond strength between the adjacent layers (delamination Fig. 6.b).This is probably due to the difference in chemical properties of both materials or immiscibility William et al. (2021), high crystallinity (Verma et al., 2023) and the large volume of the object as delamination issues were more visible at the time of print the chair that in the parameters optimization process. Indeed, delamination presented in the printing of a larger object can be attributed to the rapid cooling of the layers before the material is once again deposed contrary of the cube printing where the small surface allowing the adhesion of layers before there are completely cooled. This can even be an issue for more popular 3-D printing materials like PLA from the print surface (Wijnen et al., 2018). The addition of agents that reduce the interphase tension between polymers might help to solve the delamination present and enhance the properties of the material (Dai et al., 1997; Inoya et al., 2012; Kramer et al., 1994) as interfacial bond can be enhanced by polymer modification (Gao et al., 2021) and viscosity decrement (Ko et al., 2019). Additionally, while printing warping problems were observed, (Fig. 6.c) which are likely caused by the high crystallization rates of HDPE (Schirmeister et al., 2019) suggesting that the incorporation of this plastic even in a low portions have affected the printing negatively. The use of Magigoo (**https://magigoo.com?**/) and the addition of a brim was tested in order to enable bed adhesion, yet this solutions did not completely solve the problem. A previous study showed that the use of a building plate made of thermoplastic elastomer SEBS allowed the adhesion of the plastic and enables facile detachments of the printing object without breaking or damaging (Schirmeister et al., 2019), suggesting a solution that needs further evaluation in future work. Another visible issue present in the close angles of the printed object was the shrinkage (Fig. 6.d) which

occurs during solidification and especially upon polymer crystallization. Moreover, as is well-know, PET has hygroscopic tendencies and easily absorbs atmosphere moisture making it difficult to extrude (Bustos Seibert et al., 2022) thus is likely to break down in the presence of water, lowering the quality of the print. Before the chair printing some samples showed brittle behavior and voids formation therefore, the material was constantly dried and the hopper was closed in order to avoid moisture coming from the environment helping to have a more printable material. Visually it can be observed some vibration and ringing problems (Fig. 6.e) caused by the machine upgrading, both acceleration and jerk (maximum value of the instantaneous speed change) needs finer tuning.
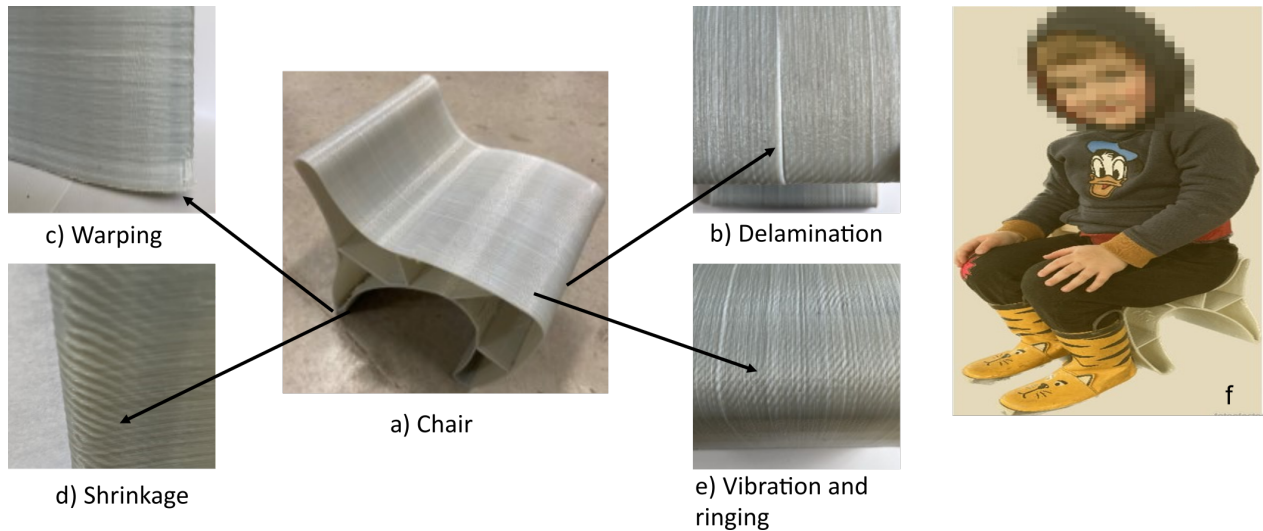

c) Warping

b) Delamination

a) Chair

d) Shrinkage

e) Vibration and ringing

f

Figure 7: Finished children chair and printing issues

3.7.1 Cost and environmental impact

The printing time took 10 h and the printed object has a mass of 840 g. Due to the found optimized speed being low, the printing rate (grams per hour) is low considering the machine that pellet printers have a typical throughput of 220 g to 9 kg per hour. The printing time could be improved by upgrading the extruder motor to a more powerful one. Besides, the energy required for 10 hr of 3-D printing was found to be 6 kW-hr resulting in a production cost of ~1.2 € in function of the electricity cost in France, without considering the material cost as bottles were obtained from post-consumers waste. When labor costs

are not included the price was significative reduced (~88%) compared with those low cost found in the market [@ https://www.ikea.com/fr/fr/p/mammut-tabouret-enfant-interieur-exterieur-jaune-20382324].

The economics of fabricating the case study product remained competitive even if recycled plastic pellets or shreds are used, which can be found on the market from 1-10 €/kg. However, labor, maintenance and machine devaluation were not considered in the final price and are needed in future work for a complete economic evaluation.

Regarding the environmental impact, although this study does not evaluate the entire life cycle of the printed object, various scientific studies have already shown feasibility of distributed recycling (Kerdlap et al., 2022; Santander et al., 2020), the comparation between conventional and distributed manufacturing in terms of energy consumption and emissions (Kreiger and Pearce, 2013), environmental performance of AM Colorado et al. (2020) and the appearance of DRAM as a source of raw material for diverse 3-D printers coming from post-consumer plastic waste in the form of either filament (Hart et al., 2018; Mikula et al., 2021; Mohammed et al., 2017b; Pakkanen et al., 2017b) or granules (Alexandre et al., 2020).

Additionally, Caceres-Mendoza et al. (2023) has developed a complete life of cycle assessment of a DRAM system based on the production of PLA filament comparing virgin and recycled materials. Their environmental results showed a reduction of the impacts of production (climate change, fossil depletion, water depletion and potential eutrophication) of ~97% compared to virgin filament. These results, however, are dependent on the energy supply and can vary depending on location.

4   Conclusion and future work

This study analyzed the feasibility of using mixed post-consumer waste as feedstock material for direct 3-D printing without compatibilization. The results showed the potential of mixing solid waste plastics (PET/HDPE) for its use as feedstock material by printing a water bottle with two incompatible polymers from the cap and body of the bottle. Additionally, the results

showed that a large-scale FGF 3-D printer was capable of producing a cost-effective functional object from these mixed waste PET/HDPE plastics. Further research is needed in the analysis of mechanical properties of the material as well as the possibilities of using compatibilizers capable of enhancing the interphase tension between plastics and lower their crystallinity, which might help improve performance and enhance material and 3-D printed part properties. These factors increase in importance as the scale of the 3-D printed part increases. The improvement of the material science of the approach can also offer an opportunity to improve the quality of the printing printing time, lowering the energy consumption of the machine and thus improving the economic viability of DRAM with mixed plastic waste.

In addition, future work could assess the different types of combinations or blends between commodity plastics using or not compatibilizer towards its printability, bringing out the possibility of selection/sorting process elimination. In the same way, the development of a methodology that allows the reproducibility of the process even in areas with limited infrastructure opens up the potential of plastic revalorization using DRAM.

Declaration of competing

The authors declare that they have no known competing financial interest or personal relationships that could have appeared to influence the work reported in this paper. Acknowledgements

Acknowledgements

References

Alexandre, A., Cruz Sanchez, F.A., Boudaoud, H., Camargo, M., Pearce, J.M., 2020. Mechanical Properties of Direct Waste Printing of Polylactic Acid with Universal Pellets Extruder: Comparison to Fused Filament Fabrication on Open-Source Desktop Three-Dimensional Printers. 3D Printing and Additive Manufacturing 7, 237–247. https://doi.org/10.1089/3dp.2019.0195

Anderson, I., 2017. Mechanical Properties of Specimens 3D Printed with Virgin and Recycled Polylactic Acid. 3D Printing and Additive Manufacturing 4, 110–115. https://doi.org/10.1089/3dp.2016.0054

Asadi-Eydivand, M., Solati-Hashjin, M., Fathi, A., Padashi, M., Abu Osman, N.A., 2016. Optimal design of a 3D-printed scaffold using intelligent evolutionary algorithms. Applied Soft Computing 39, 36–47. https://doi.org/10.1016/j.asoc.2015.11.011

Attaran, M., 2020. 3D Printing Role in Filling the Critical Gap in the Medical Supply Chain during COVID-19 Pandemic. American Journal of Industrial and Business Management 10, 988–1001. https://doi.org/10.4236/ajibm.2020.105066

Baechler, C., DeVuono, M., Pearce, J.M., 2013. Distributed recycling of waste polymer into RepRap feedstock. Rapid Prototyping Journal 19, 118–125. https://doi.org/10.1108/13552541311302978

Bowyer, A., 2014. 3D Printing and Humanity's First Imperfect Replicator. 3D Printing and Additive Manufacturing 1, 4–5. https://doi.org/10.1089/3dp.2013.0003

Bustos Seibert, M., Mazzei Capote, G.A., Gruber, M., Volk, W., Osswald, T.A., 2022. Manufacturing of a PET Filament from Recycled Material for Material Extrusion (MEX). Recycling 7, 69. https://doi.org/10.3390/recycling7050069

Byard, D.J., Woern, A.L., Oakley, R.B., Fiedler, M.J., Snabes, S.L., Pearce, J.M., 2019. Green fab lab applications of large-area waste polymer-based additive manufacturing. Additive Manufacturing 27, 515–525. https://doi.org/10.1016/j.addma.2019.03.006

Caceres-Mendoza, C., Santander-Tapia, P., Cruz Sanchez, F.A., Troussier, N., Camargo, M., Boudaoud, H., 2023. Life cycle assessment of filament production in distributed

plastic recycling via additive manufacturing. Cleaner Waste Systems 5, 100100. https://doi.org/10.1016/j.clwas.2023.100100

Carrete, I.A., Quiñonez, P.A., Bermudez, D., Roberson, D.A., 2021. Incorporating Textile-Derived Cellulose Fibers for the Strengthening of Recycled Polyethylene Terephthalate for 3D Printing Feedstock Materials. Journal of polymers and the environment.

Chen, R.S., Ab Ghani, M.H., Salleh, M.N., Ahmad, S., Tarawneh, M.A., 2015. Mechanical, water absorption, and morphology of recycled polymer blend rice husk flour biocomposites. Journal of Applied Polymer Science 132. https://doi.org/10.1002/app.41494

Chong, S., Pan, G.-T., Khalid, M., Yang, T.C.-K., Hung, S.-T., Huang, C.-M., 2017. Physical Characterization and Pre-assessment of Recycled High-Density Polyethylene as 3D Printing Material. Journal of Polymers and the Environment 25, 136–145. https://doi.org/10.1007/s10924-016-0793-4

Choong, Y.Y.C., Tan, H.W., Patel, D.C., Choong, W.T.N., Chen, C.-H., Low, H.Y., Tan, M.J., Patel, C.D., Chua, C.K., 2020. The global rise of 3D printing during the COVID-19 pandemic. Nat Rev Mater 5, 637–639. https://doi.org/10.1038/s41578-020-00234-3

Chu, J.S., Koay, S.C., Chan, M.Y., Choo, H.L., Ong, T.K., 2022. Recycled plastic filament made from post-consumer expanded polystyrene and polypropylene for fused filamant fabrication. Polymer Engineering & Science 62, 3786–3795. https://doi.org/10.1002/pen.26144

Colorado, H.A., Velásquez, E.I.G., Monteiro, S.N., 2020. Sustainability of additive manufacturing: The circular economy of materials and environmental perspectives. Journal of Materials Research and Technology 9, 8221–8234. https://doi.org/10.1016/j.jmrt.2020.04.062

Corsini, L., Aranda-Jan, C.B., Moultrie, J., 2022. The impact of 3D printing on the humanitarian supply chain. https://doi.org/10.17863/CAM.51226

Cruz Sanchez, F.A., Boudaoud, H., Camargo, M., Pearce, J.M., 2020. Plastic recycling in additive manufacturing: A systematic literature review and opportunities for the circular economy. Journal of Cleaner Production 264, 121602. https://doi.org/10.1016/j.jclepro.2020.121602

Cruz Sanchez, F.A., Boudaoud, H., Hoppe, S., Camargo, M., 2017a. Polymer recycling in an open-source additive manufacturing context: Mechanical issues. Additive Manufacturing 17, 87–105. https://doi.org/10.1016/j.addma.2017.05.013

Cruz Sanchez, F.A., Boudaoud, H., Hoppe, S., Camargo, M., 2017b. Polymer recycling in an open-source additive manufacturing context: Mechanical issues. Additive Manufacturing 17, 87–105. https://doi.org/10.1016/j.addma.2017.05.013

Dai, C.-A., Jandt, K.D., Iyengar, D.R., Slack, N.L., Dai, K.H., Davidson, W.B., Kramer, E.J., Hui, C.-Y., 1997. Strengthening Polymer Interfaces with Triblock Copolymers. Macromolecules 30, 549–560. https://doi.org/10.1021/ma960396s

Dertinger, S.C., Gallup, N., Tanikella, N.G., Grasso, M., Vahid, S., Foot, P.J.S., Pearce, J.M., 2020. Technical pathways for distributed recycling of polymer composites for distributed manufacturing: Windshield wiper blades. Resources, Conservation and Recycling 157, 104810. https://doi.org/10.1016/j.resconrec.2020.104810

Despeisse, M., Baumers, M., Brown, P., Charnley, F., Ford, S.J., Garmulewicz, A., Knowles, S., Minshall, T.H.W., Mortara, L., Reed-Tsochas, F.P., Rowley, J., 2017. Unlocking value for a circular economy through 3D printing: A research agenda. Technological Forecasting and Social Change 115, 75–84. https://doi.org/10.1016/j.techfore.2016.09.021

Evode, N., Qamar, S.A., Bilal, M., Barceló, D., Iqbal, H.M.N., 2021. Plastic waste and its management strategies for environmental sustainability. Case Studies in Chemical and Environmental Engineering 4, 100142. https://doi.org/10.1016/j.cscee.2021.100142

Fontana, L., Giubilini, A., Arrigo, R., Malucelli, G., Minetola, P., 2022. Characterization of 3D Printed Polylactic Acid by Fused Granular Fabrication through Printing Accuracy, Porosity, Thermal and Mechanical Analyses. Polymers 14, 3530. https://doi.org/10.3390/polym14173530

Ford, S., Despeisse, M., 2016. Additive manufacturing and sustainability: An exploratory study of the advantages and challenges. Journal of Cleaner Production 137, 1573–1587. https://doi.org/10.1016/j.jclepro.2016.04.150

Gaikwad, V., Ghose, A., Cholake, S., Rawal, A., Iwato, M., Sahajwalla, V., 2018. Transformation of E-Waste Plastics into Sustainable Filaments for 3D Printing. ACS Sustain-

able Chemistry & Engineering 6, 14432–14440. https://doi.org/10.1021/acssuschemeng.8b03105

Gallup, N., Bow, J.K., Pearce, J.M., 2018. Economic Potential for Distributed Manufacturing of Adaptive Aids for Arthritis Patients in the U.S. Geriatrics 3, 89. https://doi.org/10.3390/geriatrics3040089

Gao, X., Qi, S., Kuang, X., Su, Y., Li, J., Wang, D., 2021. Fused filament fabrication of polymer materials: A review of interlayer bond. Additive Manufacturing 37, 101658. https://doi.org/10.1016/j.addma.2020.101658

Garcia, F.L., Moris, V.A. da S., Nunes, A.O., Silva, D.A.L., 2018. Environmental performance of additive manufacturing process – an overview. Rapid Prototyping Journal 24, 1166–1177. https://doi.org/10.1108/RPJ-05-2017-0108

Geyer, R., 2020. Chapter 2 - Production, use, and fate of synthetic polymers, in: Letcher, T.M. (Ed.), Plastic Waste and Recycling. Academic Press, pp. 13–32. https://doi.org/10.1016/B978-0-12-817880-5.00002-5

Geyer, R., Jambeck, J.R., Law, K.L., 2017. Production, use, and fate of all plastics ever made. Science Advances 3, e1700782. https://doi.org/10.1126/sciadv.1700782

Grassi, G., Spagnolo, S.L., Paoletti, I., 2019. Fabrication and durability testing of a 3D printed façade for desert climates. Additive Manufacturing 28, 439.

Gwamuri, J., Franco, D., Khan, K.Y., Gauchia, L., Pearce, J.M., 2016. High-Efficiency Solar-Powered 3-D Printers for Sustainable Development. Machines 4, 3. https://doi.org/10.3390/machines4010003

Hart, K.R., Frketic, J.B., Brown, J.R., 2018. Recycling meal-ready-to-eat (MRE) pouches into polymer filament for material extrusion additive manufacturing. Additive Manufacturing 21, 536–543. https://doi.org/10.1016/j.addma.2018.04.011

ImageJ, 2023. Image processing and analysis in java [WWW Document]. URL https://imagej.nih.gov/ij/download.html (accessed 6.13.2023).

Inoya, H., Wei Leong, Y., Klinklai, W., Thumsorn, S., Makata, Y., Hamada, H., 2012. Compatibilization of recycled poly (ethylene terephthalate) and polypropylene blends: Effect of polypropylene molecular weight on homogeneity and compatibility. Journal of

applied polymer science 124, 3947–3955.

Jaisingh Sheoran, A., Kumar, H., 2020. Fused Deposition modeling process parameters optimization and effect on mechanical properties and part quality: Review and reflection on present research. Materials Today: Proceedings, International Conference on Mechanical and Energy Technologies 21, 1659–1672. https://doi.org/10.1016/j.matpr.2019.11.296

Jonathan GUIDIGO1, Stéphane MOLINA2, Edmond C. ADJOVI3, André MERLIN 4, DONNOT André5, Merlin SIMO TAGNE6, 2017. Polyethylene Low and High Density-Polyethylene Terephthalate and Polypropylene Blend as Matrices for Wood Flour, in: International Journal of Science and Research (IJSR). pp. 1069–1074. https://doi.org/10.21275/ART20164296

Jones, R., Haufe, P., Sells, E., Iravani, P., Olliver, V., Palmer, C., Bowyer, A., 2011. RepRap – the replicating rapid prototyper. Robotica 29, 177–191. https://doi.org/10.1017/S026357471000069X

Kerdlap, P., Purnama, A.R., Low, J.S.C., Tan, D.Z.L., Barlow, C.Y., Ramakrishna, S., 2022. Comparing the environmental performance of distributed versus centralized plastic recycling systems: Applying hybrid simulation modeling to life cycle assessment. Journal of Industrial Ecology 26, 252–271. https://doi.org/10.1111/jiec.13151

King, D., Babasola, A., Rozario, J., Pearce, J., 2014. Mobile Open-Source Solar-Powered 3-D Printers for Distributed Manufacturing in Off-Grid Communities. Challenges in Sustainability 2. https://doi.org/10.12924/cis2014.02010018

Ko, Y.S., Herrmann, D., Tolar, O., Elspass, W.J., Brändli, C., 2019. Improving the filament weld-strength of fused filament fabrication products through improved interdiffusion. Additive Manufacturing 29, 100815. https://doi.org/10.1016/j.addma.2019.100815

Kramer, E.J., Norton, L.J., Dai, C.-A., Sha, Y., Hui, C.-Y., 1994. Strengthening polymer interfaces. Faraday Discussions 98, 31–46. https://doi.org/10.1039/FD9949800031

Kratofil, L., Hrnjak-Murgić, Z., Jelenć, J., Andricć, B., Kovacć, T., Merzel, V., 2006. Study of the compatibilizer effect on blends prepared from waste poly (ethylene-terephthalate) and high density polyethylene. International Polymer Processing 21, 328–335.

Kreiger, M.a., Mulder, M.L., Glover, A.G., Pearce, J.M., 2014. Life cycle analysis of dis-

tributed recycling of post-consumer high density polyethylene for 3-D printing filament. Journal of Cleaner Production 70, 90–96. https://doi.org/10.1016/j.jclepro.2014.02.009

Kreiger, M.A., Mulder, M.L., Glover, A.G., Pearce, J.M., 2014. Life cycle analysis of distributed recycling of post-consumer high density polyethylene for 3-D printing filament. Journal of Cleaner Production 70, 90–96. https://doi.org/10.1016/j.jclepro.2014.02.009

Kreiger, M., Pearce, J.M., 2013. Environmental Impacts of Distributed Manufacturing from 3-D Printing of Polymer Components and Products. MRS Proceedings 1492, 85–90. https://doi.org/10.1557/opl.2013.319

Lei, Y., Wu, Q., Zhang, Q., 2009. Morphology and properties of microfibrillar composites based on recycled poly (ethylene terephthalate) and high density polyethylene. Composites Part A: Applied Science and Manufacturing 40, 904–912. https://doi.org/10.1016/j.compositesa.2009.04.017

Lipsky, S., Przyjemski, A., Velasquez, M., Gershenson, J., 2019. 3D Printing for Humanitarian Relief: The Printer Problem, in: 2019 IEEE Global Humanitarian Technology Conference (GHTC). pp. 1–7. https://doi.org/10.1109/GHTC46095.2019.9033053

Little, H.A., Tanikella, N.G., J. Reich, M., Fiedler, M.J., Snabes, S.L., Pearce, J.M., 2020. Towards Distributed Recycling with Additive Manufacturing of PET Flake Feedstocks. Materials 13, 4273. https://doi.org/10.3390/ma13194273

Löschke, S.K., Mai, J., Proust, G., Brambilla, A., 2019. Microtimber: The Development of a 3D Printed Composite Panel Made from Waste Wood and Recycled Plastics. Digital Wood Design 24, 827–848. https://doi.org/10.1007/978-3-030-03676-8_33

MacArthur, E., 2017. Beyond plastic waste. Science 358, 843–843. https://doi.org/10.1126/science.aao6749

Mikula, K., Skrzypczak, D., Izydorczyk, G., Warchoł, J., Moustakas, K., Chojnacka, K., Witek-Krowiak, A., 2021. 3D printing filament as a second life of waste plastics—a review. Environmental Science and Pollution Research 28, 12321–12333. https://doi.org/10.1007/s11356-020-10657-8

Mohammed, M.I., Das, A., Gomez-Kervin, E., Wilson, D., Gibson, I., 2017a. EcoPrinting: Investigating the Use of 100% Recycled Acrylonitrile Butadiene Styrene (ABS) for

Additive Manufacturing. University of Texas at Austin.

Mohammed, M.I., Mohan, M., Das, A., Johnson, M.D., Badwal, P.S., McLean, D., Gibson, I., 2017b. A low carbon footprint approach to the reconstitution of plastics into 3D-printer filament for enhanced waste reduction. KnE Engineering 234–241. https://doi.org/10.18502/keg.v2i2.621

Mohammed, M.I., Wilson, D., Gomez-Kervin, E., Rosson, L., Long, J., 2018. EcoPrinting: Investigation of Solar Powered Plastic Recycling and Additive Manufacturing for Enhanced Waste Management and Sustainable Manufacturing, in: 2018 IEEE Conference on Technologies for Sustainability (SusTech). IEEE, pp. 1–6. https://doi.org/10.1109/SusTech.2018.8671370

Nofar, M., Oğuz, H., 2019. Development of PBT/Recycled-PET Blends and the Influence of Using Chain Extender. Journal of Polymers and the Environment 27, 1404–1417. https://doi.org/10.1007/s10924-019-01435-w

Novak, J.I., Loy, J., 2020. A critical review of initial 3D printed products responding to COVID-19 health and supply chain challenges. Emerald Open Research 2, 24. https://doi.org/10.35241/emeraldopenres.13697.1

Oberloier, S., Whisman, N.G., Pearce, J.M., 2022a. Finding Ideal Parameters for Recycled Material Fused Particle Fabrication-Based 3D Printing Using an Open Source Software Implementation of Particle Swarm Optimization. 3D Printing and Additive Manufacturing. https://doi.org/10.1089/3dp.2022.0012

Oberloier, S., Whisman, N.G., Pearce, J.M., 2022b. Finding Ideal Parameters for Recycled Material Fused Particle Fabrication-Based 3D Printing Using an Open Source Software Implementation of Particle Swarm Optimization. 3D Printing and Additive Manufacturing. https://doi.org/10.1089/3dp.2022.0012

Pakkanen, J., Manfredi, D., Minetola, P., Iuliano, L., 2017a. About the Use of Recycled or Biodegradable Filaments for Sustainability of 3D Printing, in: Campana, G., Howlett, R.J., Setchi, R., Cimatti, B. (Eds.),. Springer International Publishing, Cham, pp. 776–785. https://doi.org/10.1007/978-3-319-57078-5_73

Pakkanen, J., Manfredi, D., Minetola, P., Iuliano, L., 2017b. About the Use of Recycled or

Biodegradable Filaments for Sustainability of 3D Printing, in: Campana, G., Howlett, R.J., Setchi, R., Cimatti, B. (Eds.), Sustainable Design and Manufacturing 2017, Smart Innovation, Systems and Technologies. Springer International Publishing, Cham, pp. 776–785. https://doi.org/10.1007/978-3-319-57078-5_73

Pan, Y., Wu, G., Ma, H., Zhou, S., Zhang, H., 2020. Improved compatibility of PET/HDPE blend by using GMA grafted thermoplastic elastomer. Polymer-Plastics Technology and Materials 59, 1887–1898.

Pearce, J., Qian, J.-Y., 2022. Economic Impact of DIY Home Manufacturing of Consumer Products with Low-cost 3D Printing from Free and Open Source Designs. European Journal of Social Impact and Circular Economy 3, 1–24. https://doi.org/10.13135/2704-9906/6508

Petersen, E., Kidd, R., Pearce, J., 2017. Impact of DIY Home Manufacturing with 3D Printing on the Toy and Game Market. Technologies 5, 45. https://doi.org/10.3390/technologies5030045

Petsiuk, A., Lavu, B., Dick, R., Pearce, J.M., 2022. Waste Plastic Direct Extrusion Hangprinter. Inventions 7, 70. https://doi.org/10.3390/inventions7030070

Pringle, A.M., Rudnicki, M., Pearce, J.M., 2018. Wood Furniture Waste–Based Recycled 3-D Printing Filament. Forest Products Journal 68, 86–95. https://doi.org/10.13073/FPJ-D-17-00042

Raju, M., Gupta, M.K., Bhanot, N., Sharma, V.S., 2019. A hybrid PSO–BFO evolutionary algorithm for optimization of fused deposition modelling process parameters. Journal of Intelligent Manufacturing 30, 2743–2758. https://doi.org/10.1007/s10845-018-1420-0

Rattan, R.S., Nauta, N., Romani, A., Pearce, J.M., 2023. Hangprinter for large scale additive manufacturing using fused particle fabrication with recycled plastic and continuous feeding. HardwareX 13, e00401. https://doi.org/10.1016/j.ohx.2023.e00401

Reich, M.J., Woern, A.L., Tanikella, N.G., Pearce, J.M., 2019. Mechanical Properties and Applications of Recycled Polycarbonate Particle Material Extrusion-Based Additive Manufacturing. Materials 12, 1642. https://doi.org/10.3390/ma12101642

Rett, J.P., Traore, Y.L., Ho, E.A., 2021. Sustainable Materials for Fused Deposition Modeling

3D Printing Applications. Advanced Engineering Materials 23, 2001472. https://doi.org/10.1002/adem.202001472

Romani, A., Rognoli, V., Levi, M., 2021. Design, Materials, and Extrusion-Based Additive Manufacturing in Circular Economy Contexts: From Waste to New Products. Sustainability 13, 7269. https://doi.org/10.3390/su13137269

Roschli, A., Gaul, K.T., Boulger, A.M., Post, B.K., Chesser, P.C., Love, L.J., Blue, F., Borish, M., 2019. Designing for Big Area Additive Manufacturing. Additive Manufacturing 25, 275–285. https://doi.org/10.1016/j.addma.2018.11.006

Saad, M.S., Nor, A.M., Baharudin, M.E., Zakaria, M.Z., Aiman, A.F., 2019. Optimization of surface roughness in FDM 3D printer using response surface methodology, particle swarm optimization, and symbiotic organism search algorithms. The International Journal of Advanced Manufacturing Technology 105, 5121–5137. https://doi.org/10.1007/s00170-019-04568-3

Salmi, M., Akmal, J.S., Pei, E., Wolff, J., Jaribion, A., Khajavi, S.H., 2020. 3D Printing in COVID-19: Productivity Estimation of the Most Promising Open Source Solutions in Emergency Situations. Applied Sciences 10, 4004. https://doi.org/10.3390/app10114004

Santander, P., Cruz Sanchez, F.A., Boudaoud, H., Camargo, M., 2020. Closed loop supply chain network for local and distributed plastic recycling for 3D printing: A MILP-based optimization approach. Resources, Conservation and Recycling 154, 104531. https://doi.org/10.1016/j.resconrec.2019.104531

Savonen, B.L., Mahan, T.J., Curtis, M.W., Schreier, J.W., Gershenson, J.K., Pearce, J.M., 2018. Development of a Resilient 3-D Printer for Humanitarian Crisis Response. Technologies 6, 30. https://doi.org/10.3390/technologies6010030

Schirmeister, C.G., Hees, T., Licht, E.H., Mülhaupt, R., 2019. 3D printing of high density polyethylene by fused filament fabrication. Additive Manufacturing 28, 152–159. https://doi.org/10.1016/j.addma.2019.05.003

Sells, E., Smith, Z., Bailard, S., Bowyer, A., Olliver, V., 2009. RepRap: The Replicating Rapid Prototyper - maximizing customizability by breeding the means of production, in: Piller, F.T., Tseng, M.M. (Eds.), Handbook of Research in Mass Customization and

Personalization. World Scientific, pp. 568–580.

Selvam, A., Mayilswamy, S., Whenish, R., 2020. Strength Improvement of Additive Manufacturing Components by Reinforcing Carbon Fiber and by Employing Bioinspired Interlock Sutures. Journal of Vinyl and Additive Technology 26, 511–523. https://doi.org/10.1002/vnl.21766

Shah, J., Snider, B., Clarke, T., Kozutsky, S., Lacki, M., Hosseini, A., 2019. Large-scale 3D printers for additive manufacturing: Design considerations and challenges. The International Journal of Advanced Manufacturing Technology 104, 3679–3693. https://doi.org/10.1007/s00170-019-04074-6

Shirmohammadi, M., Goushchi, S.J., Keshtiban, P.M., 2021. Optimization of 3D printing process parameters to minimize surface roughness with hybrid artificial neural network model and particle swarm algorithm. Progress in Additive Manufacturing 6, 199–215. https://doi.org/10.1007/s40964-021-00166-6

Siltaloppi, J., Jähi, M., 2021. Toward a sustainable plastics value chain: Core conundrums and emerging solution mechanisms for a systemic transition. Journal of Cleaner Production 315, 128113. https://doi.org/10.1016/j.jclepro.2021.128113

Soares, J., Miguel, I., Venâncio, C., Lopes, I., Oliveira, M., 2021. Public views on plastic pollution: Knowledge, perceived impacts, and pro-environmental behaviours. Journal of Hazardous Materials 412, 125227. https://doi.org/10.1016/j.jhazmat.2021.125227

Taghavi, S.K., Shahrajabian, H., Hosseini, H.M., 2018. Detailed comparison of compatibilizers MAPE and SEBS-g-MA on the mechanical/thermal properties, and morphology in ternary blend of recycled PET/HDPE/MAPE and recycled PET/HDPE/SEBS-g-MA. Journal of Elastomers & Plastics 50, 13–35.

Van de Voorde, B., Katalagarianakis, A., Huysman, S., Toncheva, A., Raquez, J.-M., Duretek, I., Holzer, C., Cardon, L., Bernaerts, K., V, Van Hemelrijck, D., Pyl, L., Van Vlierberghe, S., 2022. Effect of extrusion and fused filament fabrication processing parameters of recycled poly(ethylene terephthalate) on the crystallinity and mechanical properties. Additive Manufacturing 50. https://doi.org/10.1016/j.addma.2021.102518

Vaucher, J., Demongeot, A., Michaud, V., Leterrier, Y., 2022. Recycling of Bottle Grade

PET: Influence of HDPE Contamination on the Microstructure and Mechanical Performance of 3D Printed Parts. Polymers 14, 5507. https://doi.org/10.3390/polym14245507

Verma, N., Awasthi, P., Gupta, A., Banerjee, S.S., 2023. Fused Deposition Modeling of Polyolefins: Challenges and Opportunities. Macromolecular Materials and Engineering 308, 2200421. https://doi.org/10.1002/mame.202200421

Wijnen, B., Sanders, P., Pearce, J.M., 2018. Improved model and experimental validation of deformation in fused filament fabrication of polylactic acid. Progress in Additive Manufacturing 3, 193–203. https://doi.org/10.1007/s40964-018-0052-4

William, L.J.W., Koay, S.C., Chan, M.Y., Pang, M.M., Ong, T.K., Tshai, K.Y., 2021. Recycling Polymer Blend made from Post-used Styrofoam and Polypropylene for Fuse Deposition Modelling. Journal of Physics: Conference Series 2120, 012020. https://doi.org/10.1088/1742-6596/2120/1/012020

Woern, A.L., McCaslin, J.R., Pringle, A.M., Pearce, J.M., 2018. RepRapable Recyclebot: Open source 3-D printable extruder for converting plastic to 3-D printing filament. HardwareX 4, e00026. https://doi.org/10.1016/j.ohx.2018.e00026

Wong, J.Y., 2015. Ultra-Portable Solar-Powered 3D Printers for Onsite Manufacturing of Medical Resources. Aerospace Medicine and Human Performance 86, 830–834. https://doi.org/10.3357/AMHP.4308.2015

Zander, N.E., Gillan, M., Burckhard, Z., Gardea, F., 2019. Recycled polypropylene blends as novel 3D printing materials. Additive Manufacturing 25, 122–130. https://doi.org/10.1016/j.addma.2018.11.009

Zander, N.E., Gillan, M., Lambeth, R.H., 2018. Recycled polyethylene terephthalate as a new FFF feedstock material. Additive Manufacturing 21, 174–182. https://doi.org/10.1016/j.addma.2018.03.007

Zhang, Y., Wang, S., Ji, G., 2015. A Comprehensive Survey on Particle Swarm Optimization Algorithm and Its Applications. Mathematical Problems in Engineering 2015, e931256. https://doi.org/10.1155/2015/931256

Zhong, S., Pearce, J.M., 2018. Tightening the loop on the circular economy: Coupled distributed recycling and manufacturing with recyclebot and RepRap 3-D printing. Re-

sources, Conservation and Recycling 128, 48–58. https://doi.org/10.1016/j.resconrec.2017.09.023